View metadata, citation and similar papers at core.ac.uk

brought to you by CORE

provided by DigitalCommons@University of Nebraska

University of Nebraska - Lincoln

DigitalCommons@University of Nebraska - Lincoln

Faculty Publications from the Department of Electrical and Computer Engineering

Electrical & Computer Engineering, Department of

2-15-1995

InP optical constants between 0.75 and 5.0 eV determined by variable-angle spectroscopic ellipsometry

C. M. Herzinger
University of Nebraska-Lincoln

Paul G. Snyder
University of Nebraska-Lincoln, psnyder1@unl.edu

B. Johs
J. A. Woollam Co.

John A. Woollam
J. A. Woollam Co., Lincoln, Nebraska, jwoollam1@unl.edu

Follow this and additional works at: https://digitalcommons.unl.edu/electricalengineeringfacpub

Part of the Electrical and Computer Engineering Commons

Herzinger, C. M.; Snyder, Paul G.; Johs, B.; and Woollam, John A., "InP optical constants between 0.75 and 5.0 eV determined by variable-angle spectroscopic ellipsometry" (1995). *Faculty Publications from the Department of Electrical and Computer Engineering*. 59.
https://digitalcommons.unl.edu/electricalengineeringfacpub/59

This Article is brought to you for free and open access by the Electrical & Computer Engineering, Department of at DigitalCommons@University of Nebraska - Lincoln. It has been accepted for inclusion in Faculty Publications from the Department of Electrical and Computer Engineering by an authorized administrator of DigitalCommons@University of Nebraska - Lincoln.

InP optical constants between 0.75 and 5.0 eV determined by variable-angle spectroscopic ellipsometry

C. M. Herzinger and P. G. Snyder
Center for Microelectronic and Optical Materials Research, and Department of Electrical Engineering, University of Nebraska, Lincoln, Nebraska 68588-0511

B. Johs and J. A. Woollam
J. A. Woollam Co., Inc., Lincoln, Nebraska 68588

(Received 11 July 1994; accepted for publication 7 November 1994)

Using variable-angle spectroscopic ellipsometry (VASE) InP optical constants for photon energies have been determined in the range from 0.75 to 5.0 eV, which includes the fundamental gap at 1.35 eV. Above 1.5 eV the results are consistent with previously measured pseudovalues from an oxide-stripped sample when a very thin residual overlayer is accounted for. They are also shown to be compatible with previously published prism measurements of refractive index below the band gap. Real and imaginary parts of the dielectric function are shown to be Kramers–Kronig (KK) self-consistent above the gap, and the KK analysis was used to extend the dielectric function below the measurement range to 0.5 eV. The assumptions underlying biased fitting of VASE data and the importance of variable-angle measurements were investigated. The detection and significance of systematic errors for general VASE data analysis were also investigated, especially with regard to fit parameter confidence limits. © *1995 American Institute of Physics.*

I. INTRODUCTION

InP is an important substrate material for high-speed electrical and optoelectronic devices. These devices are typically formed from multiple epitaxial layers of which thickness and composition must be precisely controlled. Spectroscopic ellipsometry (SE) is a very sensitive, nondestructive characterization technique for both composition and thickness,[1] provided that accurate optical constants are available.[2] As a substrate material, accurate InP optical constants are therefore essential. Previously published InP optical constants have not completely covered the band-gap region[3–8] for both the real and imaginary parts of the complex dielectric function, and ellipsometrically determined results have not been published for the below-band-gap region. We present results here for ellipsometrically determined InP optical constants for photon energies from 0.75 to 5.0 eV, including the fundamental band-gap region around 1.35 eV.

The remaining sections discuss general ellipsometric data analysis and result interpretation, and the specific case of measuring and analyzing data for an InP substrate with a native oxide. Section II presents the terminology and our general approach for analyzing variable-angle spectroscopic ellipsometry (VASE) data. Section III discusses the utility of variable-angle measurements for the case of a thin oxide on a substrate. Our interpretation of general VASE analysis results is presented in Sec. IV. Special emphasis is given to our treatment of fit parameter confidence limits. Section V describes VASE measurements taken on an InP substrate that was prepackaged for epitaxial growth. In Sec. VI, the InP substrate dielectric function, $\epsilon=\epsilon_1+i\epsilon_2$, is determined by mathematically modeling the native oxide overlayer. Comparisons are made with Aspnes and Studna's published pseudovalues,[6] published critical-point (CP) energies,[7] and published prism measured refractive index values below the band gap.[4,8] Finally, a Kramers–Kronig (KK) analysis was performed to evaluate the accuracy of the ϵ_1 values, and to extend ϵ_1 to energies below the measurement range.

II. VASE DATA ANALYSIS

The standard ellipsometric parameters ψ and Δ are related to the complex ratio of reflection coefficients for light polarized parallel p and perpendicular s to the plane of incidence.[9] This ratio is defined as

$$\rho=\frac{R_p}{R_s}=\tan(\psi)e^{i\Delta}. \quad (1)$$

The electric-field reflection coefficient at an incident angle of ϕ is defined as $R_p(R_s)$ for $p(s)$-polarized light. A useful related parameter is the pseudodielectric function given by

$$\langle\epsilon\rangle=\langle\epsilon_1\rangle+i\langle\epsilon_2\rangle=\sin^2\phi\left[1+\tan^2\phi\left(\frac{1-\rho}{1+\rho}\right)^2\right]. \quad (2)$$

For the case of an air ambient over a bare substrate with a perfectly smooth surface, the measured pseudodielectric function $\langle\epsilon\rangle$ and the intrinsic dielectric function of the substrate ϵ_{sub} are identical. Thus, ϵ_{sub} is easily measured assuming that accurate ψ and Δ values can be obtained. To determine optical constants from any more complicated sample, VASE data must be analyzed using a parametric model that is adjusted to fit the measured data.

The basic modeling procedure[10] is as follows:

(1) The model is built starting from the nominal layered structure and adding anticipated imperfections such as interface intermixing and surface oxides;
(2) this model is then parametrized, making a list of the necessary optical constants and thicknesses to fully define the model;

Downloaded 04 Dec 2007 to 129.93.17.223. Redistribution subject to AIP license or copyright; see http://jap.aip.org/jap/copyright.jsp

(3) prior to fitting, this list is broken into two complimentary subsets of adjustable, $a_1, a_2, \ldots a_P$, and fixed, $b_1, b_2, \ldots b_Q$, parameters;
(4) the fitting algorithm then matches the model calculated ψ and Δ values to the measured values by adjusting $a_1, a_2, \ldots a_P$ (this type of fitting procedure is said to be model dependent because any model chosen, even an unphysical one, will have a "best" set of fit parameters);
(5) the model and/or the set of adjustable parameters is modified until an acceptable fit is obtained.

Section IV discusses further the problem of determining the "goodness" of the fit.

The standard model for calculating ψ^{mod} and Δ^{mod} is a sequence of parallel layers with smooth interfaces and homogeneous optical constants, on a semi-infinite substrate.[9] An imperfection such as interface intermixing can be handled within these assumptions by adding additional thin layers that grade the optical constants in steps. Small scale roughness is often modeled by allowing the mixing of optical constants using an effective medium approximation.[1,11]

We use the Levenberg–Marquardt algorithm[12] to fit the model parameters by minimizing the following weighted (biased) test function:[13]

$$\xi^2 = \frac{1}{2N-M} \sum_{i=1}^{N} \left[\left(\frac{\psi_i^{\mathrm{mod}} - \psi_i^{\mathrm{exp}}}{\sigma_{\psi,i}^{\mathrm{exp}}} \right)^2 + \left(\frac{\Delta_i^{\mathrm{mod}} - \Delta_i^{\mathrm{exp}}}{\sigma_{\Delta,i}^{\mathrm{exp}}} \right)^2 \right]$$

$$= \frac{1}{2N-M} \chi^2. \quad (3)$$

The number of measured ψ and Δ pairs is N, and the total number of real valued fit parameters is M. The two weighting parameters, $\sigma_{\psi}^{\mathrm{exp}}$ and $\sigma_{\Delta}^{\mathrm{exp}}$ (the standard deviations of the measured ψ and Δ), are obtained in our case using multiple revolutions of the rotating analyzer during data acquisition (Sec. V). Our fitting test function is a scaled version of the usual χ^2 quantity and therefore minimizing either value is equivalent. With the assumptions described in the following section, our test function has the property that statistically in the limit of a "good" fit, ξ^2 tends toward a value of one.

Reference 12 provides details and source code for implementing the nonlinear Levenberg–Marquardt fit procedure that attempts to minimize ξ^2 (or χ^2) by finding $a_1, a_2, \ldots a_P$ such that $\partial \xi^2 / \partial a_k = 0$ for $k = 1 \cdots P$. A key element of the fitting procedure is the curvature matrix $[\alpha]$,

$$\alpha_{kl} = \sum_{i=1}^{N} \left(\frac{1}{\sigma_{\psi,i}^2} \frac{\partial \psi_i^{\mathrm{mod}}}{\partial a_k} \frac{\partial \psi_i^{\mathrm{mod}}}{\partial a_l} + \frac{1}{\sigma_{\Delta,i}^2} \frac{\partial \Delta_i^{\mathrm{mod}}}{\partial a_k} \frac{\partial \Delta_i^{\mathrm{mod}}}{\partial a_l} \right). \quad (4)$$

The curvature matrix is related to the covariance matrix of the fit parameters by $[C] \equiv [\alpha]^{-1}$. The standard 90% confidence limit[12] (SCL) and the figure of merit (FOM) we have adopted to describe confidence in the ith fit parameter are given by

$$\mathrm{SCL}_i = 1.65 \sqrt{C_{ii}} \quad \text{and} \quad \mathrm{FOM}_i = \mathrm{SCL}_i \xi. \quad (5)$$

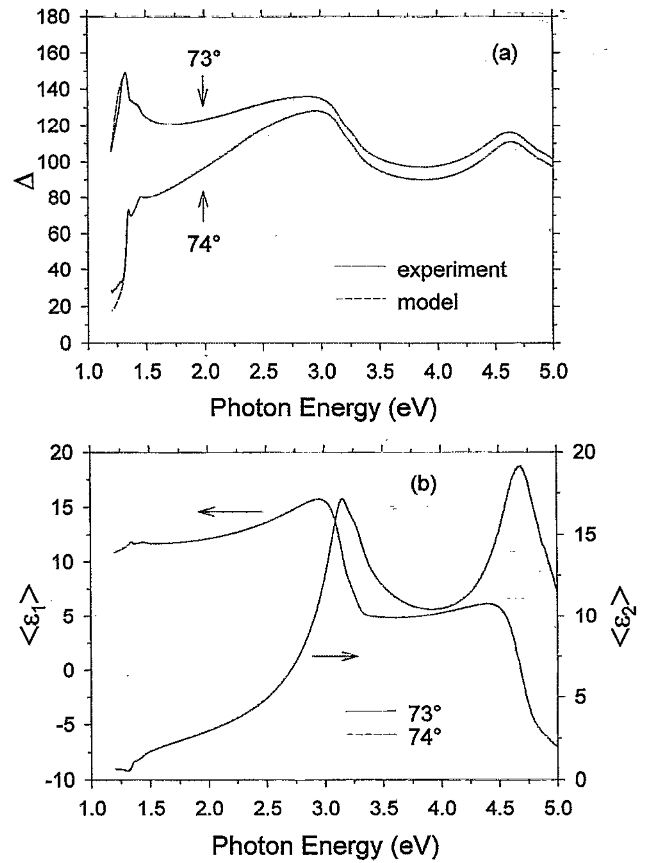

FIG. 1. (a) Δ spectra measured for two incident angles (73° and 74°) on an InP substrate with a native oxide and the model results using the final InP optical constants from Sec. VI. There is near perfect agreement above the bandgap. Below the band gap, an exponential absorption tail has been imposed on the model dielectric function. The corresponding experimental pseudodielectric functions are shown in (b). The measured pseudovalues are essentially identical for the two different angles even though the Δ spectra are quite different.

C_{ii} is the ith diagonal element of the covariance matrix. The assumptions required to accurately determine confidence limits and methods of interpreting this FOM are discussed in Sec. IV.

III. SIGNIFICANCE OF VARIABLE-ANGLE MEASUREMENTS

In this section we examine the utility of acquiring data at multiple angles of incidence. Multiple-angle measurements do not always produce the desired effect of enhancing information content. Consider the task of determining optical constants at W wavelengths of a substrate that has an overlayer of known optical properties but unknown thickness. The total number of real-valued unknowns is $2W+1$. For SE data acquired at one angle of incidence ϕ_1, the total number of measured values is $2W$, hence the system is underdetermined (fewer measured values than parameters). By measuring the sample at a second angle of incidence ϕ_2, the number of measured values increases to $4W$ and the system might appear to be over determined; however, in many cases of interest, the system still has no unique set of fit parameters be-

Downloaded 04 Dec 2007 to 129.93.17.223. Redistribution subject to AIP license or copyright; see http://jap.aip.org/jap/copyright.jsp

cause there is a strong correlation in the information content between data at different angles. This is especially true when the overlayer is thin (i.e., native oxides, surface roughness). This information correlation is easily observed in the pseudodielectric spectra as shown in the comparison between Δ spectra and $\langle\epsilon\rangle$ spectra in Fig. 1, for an InP substrate with a thin oxide overlayer. Even though the measured Δ spectra at the two angles are quite different, the $\langle\epsilon_1\rangle$ and $\langle\epsilon_2\rangle$ spectra at each angle are identical within the noise level. In this case, the second angle of incidence contributes no additional information above the measurement noise level, and therefore no additional parameters can be independently fitted.

However, multiple angles are always valuable in several ways. First, measurements at the same wavelength are independent with respect to measurement noise, and therefore the extra information helps to reduce noise in the fitted parameters. Second, the additional measurements improve the statistical determination of confidence limits by further over determining the model. Third, the proper choice of multiple angles ensures that for each wavelength, at least one pair of ψ and Δ values will be near the optimum measurement regime for the type of ellipsometer being used (e.g., a rotating-analyzer ellipsometer is most accurate for $\Delta\sim 90°$). Finally, angles may be chosen at which ψ and Δ are most sensitive to the model parameters.[14] For an absorbing substrate with only a very thin overlayer, this also occurs when $\Delta\sim 90°$.

IV. INTERPRETATION OF CONFIDENCE LIMITS

Determining appropriate confidence limits for the fit parameters can be a confusing issue because many assumptions are used in transforming the experimental uncertainties into fit parameter error bars. This section discusses the validity of these assumptions and the appropriate interpretation of confidence limits when the assumptions may be violated. The basic assumptions are as follows:

(1) Measured ψ and Δ values are independent, normally distributed random variables, and accurate standard deviations of the measured quantities, σ_ψ^{exp} and σ_Δ^{exp}, are available;
(2) the final fit is good, in that the differences between the model-calculated values and the experimental values are random with a normal distribution and the same deviations as the measured values;
(3) the derivatives in Eq. (4) are valid over a wide enough range that the experimental deviations can be linearly mapped over to the fit parameter deviations;
(4) correlations between the fit parameters are small enough that individual standard deviations can be assigned.

(1) The usual assumption of normally distributed random measurement errors is made because a χ^2 minimization assumes it.[12] In fact, this may be a reasonable approximation even for complicated measurement quantities such as ψ and Δ, but it can not be universally true. For example, a normally distributed error in ψ is impossible if $\psi_{true}\rightarrow 0$, since $\psi_{meas}\geqslant 0$. In addition, confidence limit accuracy is directly related to the accuracy of σ_ψ^{exp} and σ_Δ^{exp}. For a rotating-analyzer ellipsometer, these values can be approximately measured using multiple analyzer revolutions. (Data are averaged over multiple revolutions in any case, to improve the signal-to-noise ratio.) Note that for a biased fitting procedure, only the relative magnitude of the standard deviations is important; relatively noisy spectral regions ($\Delta\approx 0°$, 180°, or low light intensity) contribute less to the overall fit. If all the measurement standard deviations are scaled by the same amount, the same final set of fit parameters will be obtained, but the resulting calculated SCL will change. This is in contrast to our FOM which would remain unchanged. Certainly, relatively weighted σ_ψ^{exp} and σ_Δ^{exp} can be found for proper biased fitting, and with increasing measurement time, increasing absolute accuracy for σ_ψ^{exp} and σ_Δ^{exp} can be obtained. The assumptions of normal distributions for, and independence of, all ψ and Δ measurements are difficult to prove when acquiring a large amount of data; however, our experience is that whatever assumptions are made about measurement errors, the analysis (fitting), described next, is the larger problem.

(2) The most questionable assumption is that the differences between experimental and calculated model values are normally distributed with the same standard deviations as the measurement process. The normal distribution assumption implies that there are no systematic errors in either the measurement process or in the parametric model. The acquired standard deviations deal only with measurement precision. Calibration errors, incident angle errors, monochromator offsets, finite optical bandwidth, detector nonlinearity, etc., are systematic errors and should not be mixed with the random noise errors. These systematic acquisition errors must either be reduced to insignificance (by improving the hardware) or included in the model calculation (by fitting a correction term such as the angle of incidence). The hardware correction is, of course, preferable, since the correction term may be impossible to calculate or the term may be correlated to other more desired parameters being fit. Other systematic errors, unrelated to measurement accuracy, appear due to incorrect model assumptions about fixed optical constants, interface quality, thickness uniformity, etc. (One cannot fit for every possible model or measurement imperfection simultaneously.) Systematic model errors include propagated errors from previous optical constant measurements, and therefore may be more important than acquisition errors.

Systematic errors severely limit an objective determination of the goodness of fit based on the normal distribution assumption. If random measurement errors really are dominant then the good fit limit of our test function is $\xi^2\rightarrow 1$; however, this statistical test relies heavily on the absolute accuracy of the experimental standard deviations. If the standard deviations are scaled improperly, then unrealistic low (or high) test function values can be obtained. As pointed out earlier, however, an improper scaling does not change the final fit parameter values. If the standard deviations used are not directly acquired from the measurement process, then no objective goodness of fit is available. In any case, the final minimized ξ^2 for a particular fit can be used in a relative sense when comparing results between fits with similar models and measurement conditions.

There are some simple tests for the presence of systematic errors based on the idea that, when random measurement

Downloaded 04 Dec 2007 to 129.93.17.223. Redistribution subject to AIP license or copyright; see http://jap.aip.org/jap/copyright.jsp

errors are dominant, the experimental data will tend to be randomly above and below the model fit. No localized spectral region should contribute excessively to the test function ξ^2; however, in our experience, the vast majority of fits to SE data, have some spectral regions that fit less well than others, where the experimental values tend to be either all above or all below the model fit.[15] Even if the total number of points above the model equals those below over the whole spectrum, these groupings by wavelength are statistically so improbable that they must indicate systematic errors not accounted for in the model. A more objective test for the presence of systematic errors is to acquire two spectroscopic scans at different signal integration times. Measure ψ, Δ, and the standard deviations, and then perform the same biased fit with both spectra. If both fits produce the same overall ξ^2, then the assumption of random errors dominating is probably acceptable. (This does not imply, however, that the standard deviations have the correct absolute magnitude for confidence limit calculations.) If ξ^2 decreases as the integration time decreases, then systematic errors are dominant at long integration times when random errors are reduced by averaging. For shorter integration times random noise dominates, leading to a ξ^2 closer to the ideal value of one. The consequences of systematic errors are that the confidence limits determined using the normal error distribution assumption are not accurate, and that the usual χ^2 goodness-of-fit test indicates the model is very unlikely.[12] This second point is exactly correct though, because systematic errors by definition imply that the model is incomplete. This, however, should not mask what may be an excellent set of model parameters, accounting for all of the important spectral features except for limited regions with systematic errors. The sheer complexity of fitting SE data makes a completely objective goodness-of-fit determination problematic.

(3) The linearity of the transform from experimental errors to parameter confidence limits is less of a problem. For very noisy experimental data this assumption may be violated, but the analysis is not very meaningful in that case anyway. The experimental deviations can in principle be reduced arbitrarily by increasing measurement time. Thus, this assumption does not impose a fundamental limitation.

(4) Assigning an independent confidence limit to a fit parameter does require that the parameter be uncorrelated. This is usually a simple matter of checking the two-parameter correlation coefficients given by

$$r_{jk}=\frac{C_{jk}}{\sqrt{C_{jj}}\sqrt{C_{kk}}}. \tag{6}$$

An absolute value of r_{jk} near 1 indicates correlation between the jth and kth fit parameters. The correlation coefficients, computed from the same covariance matrix as the confidence limits,[12] are much less dependent on the absolute magnitude of the standard deviations, because those terms tend to cancel in the ratio. Thus the correlation coefficient can be objectively evaluated even when the confidence limit cannot. This two-parameter correlation check may not, however, reveal a correlation that involves three or more parameters.

From our experience of fitting SE data, we have adopted a FOM as defined in Eq. (5) to describe our confidence in the fit parameter. We specifically reserve the use of "confidence limit" to cases when all the necessary assumptions can be proved true. In those cases, our FOM reduces to the usual SCL anyway. Mathematically, the inclusion of ξ in Eq. (5) has the effect of rescaling the standard deviations such that differences between the final model and the experimental values could have been due to random errors. Unlike other examples where the standard deviations are defined after an unbiased fit,[16] our procedure includes the proper relative weighting between ψ and Δ, and among data pairs throughout the spectral region. Only at the end are the standard deviations rescaled, and then in a manner that leaves the final fit parameters unchanged.

Whereas confidence limit implies a direct connection to the sample under study, our FOM is more properly interpreted as describing the combined measurement and fitting process. Our FOM combines information about the sharpness of the fit minimum (C_{ii}) and the overall quality of the fit (ξ^2). Our FOM does give useful information when comparing fit parameters from within a single fit, or when comparing the fits from samples measured and analyzed in the same way. These are two important cases where our FOMs are quite useful on a relative basis, if not in absolute magnitude. When fitting multiple parameters from a single set of data one can correctly compare the FOM of two uncorrelated parameters to determine which is more sensitive to the data. For example, a 5 nm surface oxide thickness will have a much smaller FOM than will the thickness of a nominal 5 nm layer of material A buried below 100 nm of material B in the same sample. In this case, the ratio of FOMs is a useful number. A second example of FOM utility is in the case of quality control for a group of samples with nominally the same structure measured under the same conditions. For example, if the last sample in a series of optical coatings indicates a change of 50% in thickness over a well-established baseline value and the confidence limit as a percentage is unchanged, one can believe the fit for thickness rather than suspect an error in the measurement/fitting procedure. The real test of obtaining "true" (absolutely scaled) confidence limits from the FOM would require a great deal of work with many data analyses on samples well characterized in other ways.

V. EXPERIMENT

An ACROTEC (Japan Energy Corporation) 2 in. InP wafer with an unpolished back surface was measured using VASE. The substrate was produced by the liquid-encapsulated Czechrolski process and was Fe doped to a resistivity greater than 10^6 Ω cm. No attempt was made to remove the native oxide by chemically treating or polishing the surface. Ellipsometric measurements were made for photon energies from 0.75 to 5.0 eV using a J. A. Woollam Co., spectroscopic ellipsometer. A rotating-analyzer system was used;[6,7] however, our measurements were made at multiple and more optimal angles of incidence.[14] Also, a tracking polarizer (polarizer set near ψ) was used to keep the reflected beam close to circularly polarized. For a rotating-analyzer ellipsometer, measurement accuracy for the standard parameters ψ and Δ is best for $\Delta \sim 90°$ which occurs at the principal

Downloaded 04 Dec 2007 to 129.93.17.223. Redistribution subject to AIP license or copyright; see http://jap.aip.org/jap/copyright.jsp

TABLE I. Experimental ranges, resolutions, and angles.

E (eV)	Step size (eV)	Incident angles (deg)
0.75–1.2	0.005	72.5, 73, 73.5
1.2–1.7	0.002	73, 73.5, 74
1.7–5.1	0.010	73, 73.5, 74

angle of incidence ϕ_p. Furthermore, the data are generally most sensitive to model parameters at ϕ_p.[14] Therefore, for high accuracy over the entire spectral range and high resolution around the band gap, data acquisition was split into three ranges (Table I) with different energy resolutions and angles of incidence ϕ. Multiple angles of incidence were used but, as described in Sec. III for a substrate with a thin overlayer, data acquired at different angles are insufficient to independently determine the substrate dielectric function and the overlayer thickness. In this case, data acquired at different angles are independent with respect to measurement noise; however, they are correlated in information content. Multiple angles do help average out measurement noise, and they do insure that for each measurement wavelength at least one pair of ψ and Δ has $\Delta \sim 90°$.

The finest energy resolution was used near the band gap to resolve the E_0 and $E_0+\Delta_0$ critical points (CPs). The monochromator bandwidth was ≈ 2 nm, so the data in the middle range are not fully wavelength independent, but the close spacing is useful in later derivative calculations for CP energy determination. A small band from 0.86 to 0.93 eV was removed from the measured data due to an absorption band in the optical fiber of the light source. Remeasurement of that band with a different fiber was deemed unnecessary because the InP optical constants are very smooth in that region, well below the band gap.

VI. InP DATA ANALYSIS AND DISCUSSION

The InP data presented here were analyzed assuming an air-oxide-substrate model. The oxide optical constants were taken from a published model for InP oxide.[17] Using that parametric model, the optical constants were extended from 1.5 down to 0.75 eV. With the oxide optical constants fixed the adjustable fit parameters were the substrate optical constants and the oxide thickness t_{ox}. Ideally one would prefer to simultaneously determine t_{ox} and the InP dielectric function, however, the information content of multiple-angle data is insufficient to achieve this. Therefore, additional model assumptions or additional independent data are needed to determine t_{ox}. Ellipsometric measurements on additional wafers would not contribute much additional information unless the oxide thickness was notably different; however, for standard epitaxy-ready substrates, such as that studied here, the oxide will be consistently thin and attempts to increase this thickness (or remove it) would add an unknown degree of roughness. With t_{ox} held fixed, the InP substrate dielectric function can be readily obtained by fitting the ellipsometric data on a wavelength-by-wavelength basis. Thus, each assumed value for t_{ox} defines a slightly different possible InP dielectric function.[18] The remainder of this section describes three different approaches to determining t_{ox}.

TABLE II. Criteria used to determine oxide thickness.

Criterion	Resulting t_{ox} (nm)	FOM (t_{ox}) (nm)
Use Aspnes and Studna's pseudovalues and fit t_{ox} using data from 1.5 to 5.0 eV	1.80	0.008
Force ϵ_2 to zero at 1.306 eV	2.18	not fit
Match published absorption coefficient in the interval from 1.37 to 1.38 eV	2.02	0.003

Other approaches to determining semiconductor optical constants have involved chemically etching and polishing a substrate in an oxygen-free atmosphere.[6] Direct use of the pseudodielectric spectra determined in this way has been eminently successful for modeling more complicated semiconductor layered structures studied by ellipsometry.[14] (Using published pseudovalues $\langle\epsilon\rangle$ as intrinsic values ϵ_{sub} incorporates an assumption of zero overlayer thickness.) This surface preparation procedure is quite complicated, and a very thin residual oxide or roughened damage layer may still be present. Another approach is to clean and polish the sample in an attempt to reduce the oxide overlayer thickness, and then perform a null-ellipsometer measurement below the band gap where the semiconductor is known to be transparent. (For this measurement, a null ellipsometer with a compensator is more suitable than a rotating analyzer.) Using extrapolated oxide optical constants, the thickness of the oxide can be determined and then fixed for the extraction of the semiconductor optical constants over the remaining spectrum.[19] Our approach is more similar to the second technique, in that we mathematically remove the effect of the oxide to determine the substrate optical constants; however, we made no attempt to reduce the oxide or clean the substrate. We assumed that the substrate manufacturer made the sample as smooth and clean as possible, and that cleaning attempts on our part would not remove all the oxide and would probably also roughen the sample. Table II summarizes the three criteria and corresponding oxide thicknesses we examined.

The first criterion we chose was to assume Aspnes and Studna's published pseudovalues[6] to be intrinsic InP optical constants, $\epsilon_{sub}=\langle\epsilon\rangle_{published}$. Then, by fitting our data from 1.5 to 5.0 eV, t_{ox} was determined to be 1.80(FOM$=\pm 0.008$) nm. The extremely small FOM would be seen as unphysical if directly interpreted as a "confidence limit." As described in Sec. IV, however, the FOM is a mathematical definition [Eq. (5)] best used in a relative sense. Using this criterion, the t_{ox} value of 1.8 nm should be (and is) the smallest oxide thickness that any of our criteria produces. If another criterion indicated that a smaller oxide thicknesses was correct, that criterion would also imply the unphysical result that Aspnes and Studna's sample had a residual overlayer (oxide or roughness) of negative effective thickness.

Downloaded 04 Dec 2007 to 129.93.17.223. Redistribution subject to AIP license or copyright; see http://jap.aip.org/jap/copyright.jsp

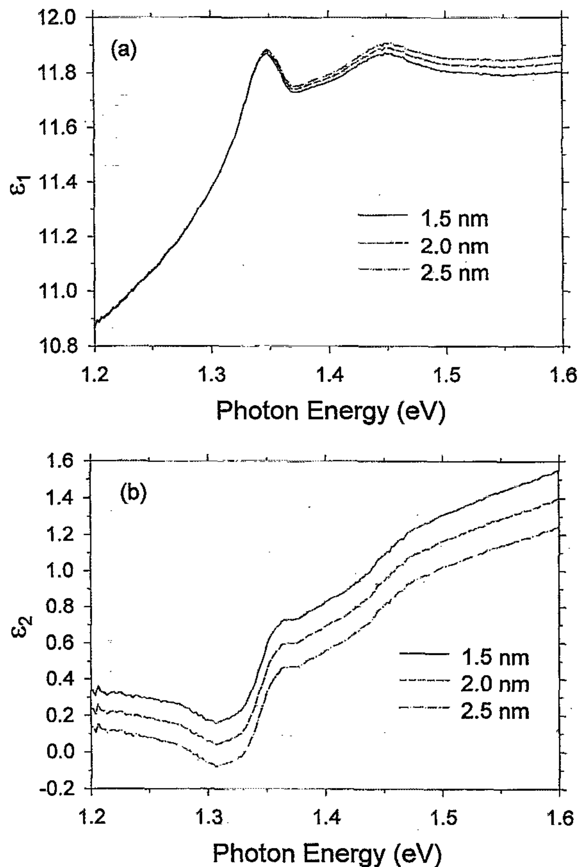

FIG. 2. Wavelength-by-wavelength conversions of the measured data into substrate dielectric functions are shown for three different assumed oxide thicknesses as indicated in the legends. Note in (a) the small influence of oxide thickness on below-gap ϵ_1 values. In (b) note the offset created by changing the model oxide thickness, but the general preservation of shape.

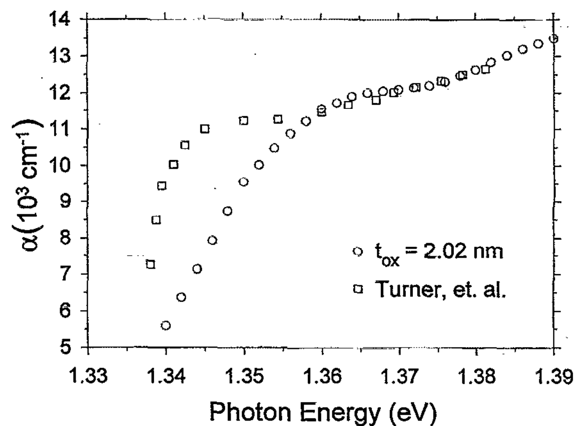

FIG. 3. Published transmission measurements of InP absorption coefficient (Ref. 3) (□) compared with our SE measurements assuming t_{ox}=2.02 nm. The oxide thickness was determined by fitting to the published values from 1.37 to 1.38 eV.

Illustrating the dependence of the results on t_{ox}, Fig. 2 shows the real and imaginary parts of the extracted InP dielectric functions, for three different assumed oxide thicknesses. Both ϵ_1 and ϵ_2 were fit over the full measurement range even though ϵ_2 should be zero below the gap. Below 1.3 eV, we see an anomalous upturn in ϵ_2 with decreasing energy, which may be due to a small amount of partially polarized light that reaches the detector after scattering from the rough backside of the sample. The rotating-analyzer ellipsometry arrangement is known to have difficulty accurately measuring Δ for low absorption (or transparent) substrates; it performs best for a beam that is circularly polarized after reflection; however, for a pure dielectric with only a very thin overlayer this occurs near the principal angle with an input polarizer setting that causes near total transmission of the probe beam into the sample. Thus, either the reflected polarization is nearly linearly polarized and difficult to measure, or almost no light is reflected from the top surface and the data can easily be corrupted by even small levels of back surface scattering.

The oxide thickness has definite effects on the fitted ϵ_2 values on both sides of the bandgap [Fig. 2(b)], but the primary effect is to simply shift the spectrum up or down. This leaves the step height and shape at the band gap independent of t_{ox}; thus, our second criterion is the simple approach of picking t_{ox} such that ϵ_2 goes to zero at its minimum, and define the energy of that minimum as E_{cut}. Then fit ϵ_1 and ϵ_2 above E_{cut}, and fit ϵ_1 only, holding $\epsilon_2=0$, below E_{cut}. This criterion yields $t_{ox}=2.18$ nm with ϵ_2 going to zero at $E_{cut}=1.306$ eV. The below-gap upturn in ϵ_2 prevents an objective, independent determination that the step height is correct; however, under the assumption that back-surface scattering produces the anomalous upturn which limits our ability to measure the full step height in ϵ_2, this criterion establishes an upper limit on the possible oxide thickness. Assuming $t_{ox}>2.18$ nm would produce a smaller step in ϵ_2 referenced to 0, or it would require the unphysical result that $\epsilon_2<0$ over part of the spectrum.

Our third criterion makes use of previously published absorption measurements for energies just above the band gap.[3] In this case, the oxide thickness was found by fitting t_{ox} and $n(E)$, while holding $k(E)$ fixed to published absorption values, in the range from 1.37 to 1.38 eV. This is essentially identical to the method used by Jellison to determine Si optical constants.[20] The values n and k are the real and imaginary parts of the complex refractive index which is related to the dielectric function by $n+ik=\sqrt{\epsilon_1+i\epsilon_2}$. This representation was used since the published absorption values are directly proportional to k, not ϵ_2. The fitting procedure yielded $t_{ox}=2.02(\pm 0.003)$ nm. This value is the one used for the extended analysis. Of the three oxide thicknesses considered we believe this one is the most appropriate, because (1) the absorption data used came from a transmission measurement which can be a very accurate technique and (2) this value falls between our other values which we already believed to be upper and lower limits on t_{ox}. With t_{ox} fixed at 2.02 nm, the InP dielectric function was fit wavelength-by-wavelength over the full measurement range, including 1.37–1.38 eV. Figure 3 compares the resulting absorption coefficient with the earlier transmission experiment. Closer to the band gap, the difference in shape might be accounted

Downloaded 04 Dec 2007 to 129.93.17.223. Redistribution subject to AIP license or copyright; see http://jap.aip.org/jap/copyright.jsp

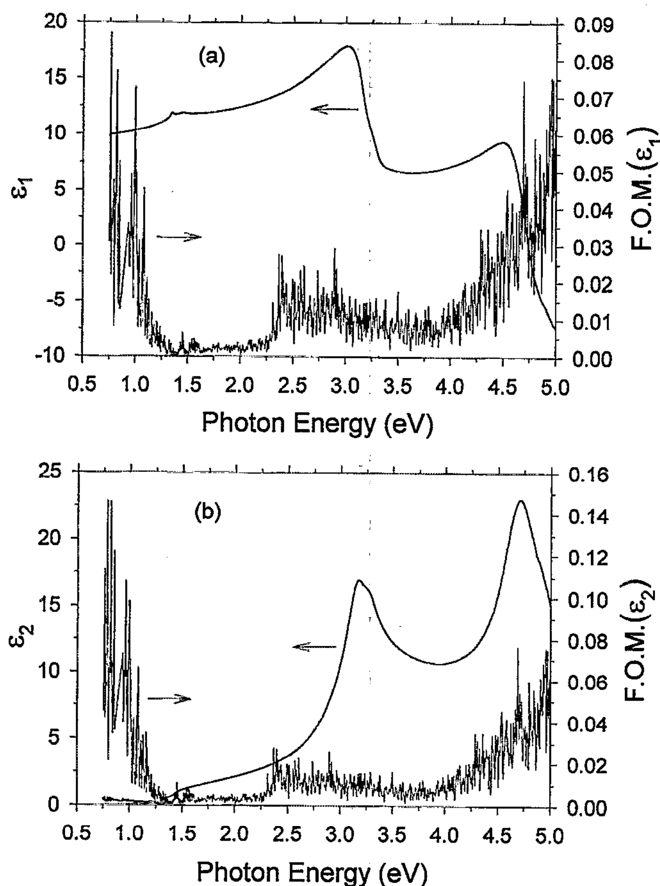

FIG. 4. Full spectra showing wavelength-by-wavelength conversion of measured data into the (a) real and (b) imaginary part of the dielectric function assuming an oxide of 2.02 nm. Also shown is the associated FOM for each value.

for by the presence of a surface electric field due to Fermi-level pinning. Transmission measurements probe the bulk material more uniformly than ellipsometry which is much more surface sensitive. The full ϵ_1 and ϵ_2 spectra are shown in Fig. 4 for t_{ox}=2.02 nm along with the confidence FOM given by Eq. (5). Since the oxide thickness was assumed (not fit), the optical constants and confidence FOM for ϵ_1 and ϵ_2 were determined on a wavelength-by-wavelength basis using the multiple angles to over determine the model. If only one angle had been used, no confidence FOM could have been calculated because the number of unknowns would have equaled the number of available data points. Individual FOM values are not very informative because at each wavelength the fitting procedure is only slightly overdetermined, and good statistics are impossible to obtain. Thus the FOM is highly variable, but certain general trends are apparent. Below the band gap, the generally larger FOM is indicative of noisier data because the substrate is transparent and very little light is reflected. The abrupt increase at 2.3 eV is due to an optical bandwidth (and intensity) reduction when a grating was changed. The data become increasingly noisy up to 5 eV because the source intensity decreases.

A more detailed look below the band gap, Fig. 5, shows that the absorption coefficient falls off approximately as an

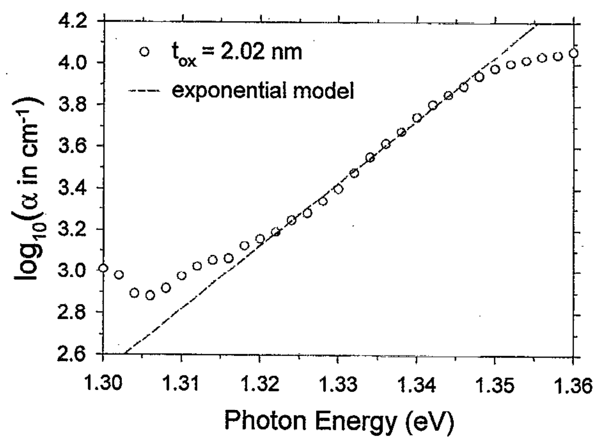

FIG. 5. Extracted absorption coefficient below the gap showing a short section of exponential decay. The model line was used to "correct" the extinction coefficient k below 1.32 eV.

exponential from 1.32 to 1.345 eV. An exponential decay is typical of either an Urbach tail or the Franz–Keldysh effect. The dashed line in Fig. 5 represents a best fit to the absorption coefficient from 1.32 to 1.345 eV, assuming an exponential dependence. Because the upturn in the extracted ϵ_2 values below 1.3 eV is attributed to an experimental artifact, the extinction coefficient k was "corrected" below 1.32 eV by extending the exponential tail as shown in Fig. 6. Then, with the new imaginary part, n was refitted in the below-gap region.

The difference in oxide thicknesses between criteria 1 and 3 (Table II) implies that a small residual overlayer, oxide, or roughness, may have been present on Aspnes and Studna's sample which was not removed by polishing. Assuming our current InP optical constants are the true intrinsic values, this thickness can be determined by first regenerating "data" (ψ and Δ values) from Aspnes and Studna's published pseudovalues at ϕ=67.08°,[6] and then fitting an overlayer thickness in the range from 1.5 to 5.0 eV. Aspnes and Stud-

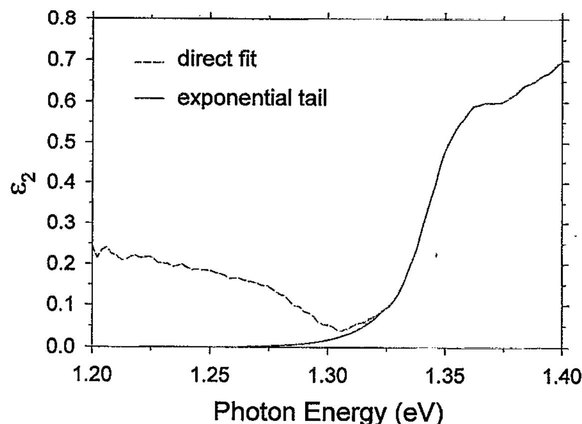

FIG. 6. Shown is the imaginary part of the dielectric function as directly determined assuming t_{ox}=2.02 nm and as modeled with the exponential absorption tail shown in Fig. 5.

Downloaded 04 Dec 2007 to 129.93.17.223. Redistribution subject to AIP license or copyright; see http://jap.aip.org/jap/copyright.jsp

TABLE III. Critical-point energies (eV) determined for InP.

	E_0	$E_0+\Delta_0$	E_1	$E_1+\Delta_1$	E'_0	$E'_0+\Delta'_0$
t_{ox}=1.50 nm	1.335	1.425	3.148	3.274	4.701	4.934
t_{ox}=2.02 nm	1.336	1.422	3.149	3.275	4.704	4.937
t_{ox}=2.50 nm	1.337	1.422	3.149	3.276	4.706	4.940
Ref. 7	1.357	1.465	3.162	3.298	4.688	4.985

na's data were found to be consistent with the current fitted t_{ox}=2.02 nm optical constants, if a 0.27(±0.013) nm oxide layer (or equivalent roughness) had been present on his sample. This thickness is comparable with the difference in the t_{ox} values from criteria (1) and (3), 0.22(2.02−1.80) nm. Because the data sets are compatible, the Aspnes and Studna data for $E>5$ eV can be used to extend our current InP dielectric function to 6 eV. Assuming a 0.27 nm residual oxide layer, the Aspnes and Studna pseudovalues from 5.0 to 6.0 eV were converted to intrinsic values compatible with this work. This was done primarily to extend ϵ_2 for the KK analysis presented later.

The CP energies were also determined by fitting the second derivative spectrum of both ϵ_1 and ϵ_2 using standard analytic line shapes,[21] including phase angles, given by the following:

$$\epsilon_1(\omega)+i\epsilon_2(\omega)=C-\sum_j A_j e^{i\phi_j}(\hbar\omega-E_j+i\Gamma_j)^{n_j}. \quad (7)$$

Table III summarizes the CP energies determined from this work and compares them with those of Ref. 7. The notation and CP orders (E_0 and $E_0+\Delta_0$: n_j=0.5; others: n_j=0.0) were taken from the same reference. The parameters for all CPs were fit simultaneously using the full spectral range. As seen from the first three rows in Table III, the assumed oxide thickness did not significantly affect the resulting CP energies. These energies and corresponding split-off band energies fall within the range of all published energies as summarized in Ref. 7. Figure 7 shows the fits to $d^2\epsilon_1/dE^2$ and $d^2\epsilon_2/dE^2$.

A KK self-consistency check was also performed. This indicated good agreement with measured values for photon energies above the band gap. The relative difference between the experimental and KK-transformed ϵ_1 values is shown in Fig. 8. The transformed ϵ_2 spectrum included the below-gap exponential tail and the appended Aspnes and Studna values for $E>5.0$ eV adjusted for 0.27 nm of oxide. To model the unmeasured absorption above 6.0 eV, an oscillator with zero broadening was added at a higher energy,

$$\epsilon_1^{KK}(\hbar\omega)=1+\frac{A_0}{E_0^2-(\hbar\omega)^2}+\frac{2}{\pi}P\int_{0.75\text{ eV}}^{6.0\text{ eV}}\frac{x\epsilon_2^{meas}}{x^2-(\hbar\omega)^2}dx. \quad (8)$$

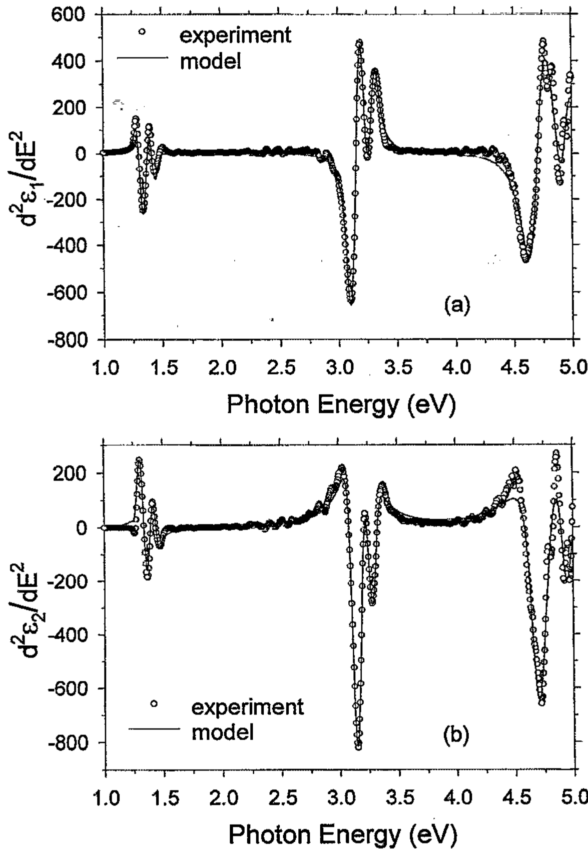

FIG. 7. Fits to the second derivative of the (a) real and (b) imaginary parts of the dielectric function using standard line-shape functions. The fit was done over the full spectral range for six critical points.

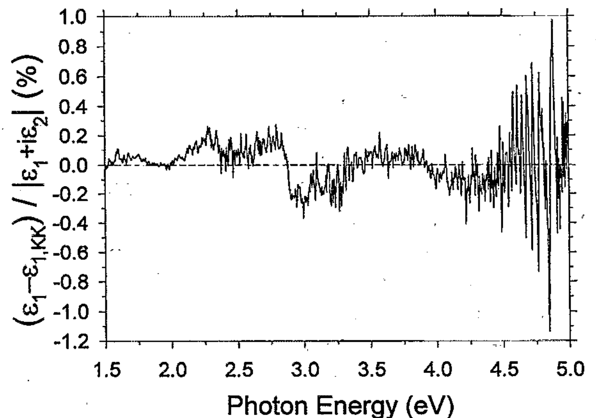

FIG. 8. Difference between the measured and the KK-modeled real part of the dielectric function. The results are plotted as a percentage of the magnitude of the dielectric function. There are some systematic errors indicated around the E_1 and $E_1+\Delta_1$ critical points.

Downloaded 04 Dec 2007 to 129.93.17.223. Redistribution subject to AIP license or copyright; see http://jap.aip.org/jap/copyright.jsp

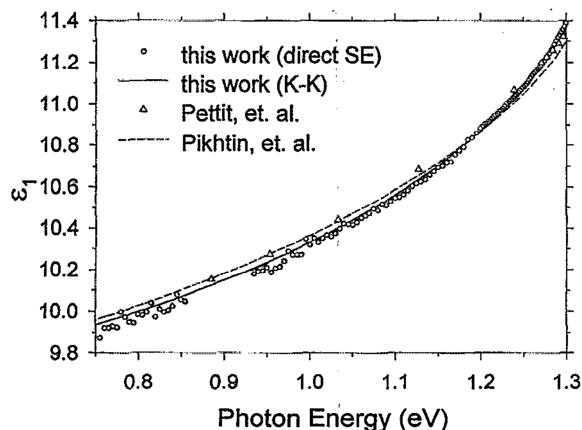

FIG. 9. The below-gap real part of the dielectric function as directly determined assuming t_{ox}=2.02 nm and after a KK analysis using the modeled exponential absorption tail is shown. These values are compared with prism measured index values (△; Ref. 4) and a model fit to below gap values (O; Ref. 8).

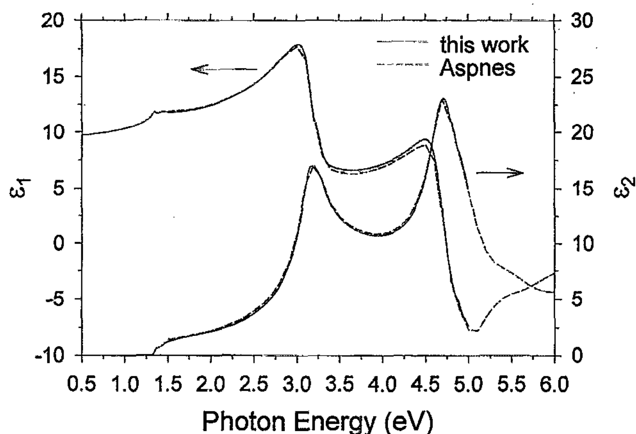

FIG. 10. Our final InP dielectric function, including an exponential absorption tail below the gap and a KK-modeled real part, is shown compared with published pseudovalues for an oxide-stripped sample (Ref. 6).

For this oscillator, the energy (E_0=7.72 eV) and magnitude (A_0=89.30 eV^2) were adjusted to fit in a least-squares manner the experimental ϵ_1 values from 1.4 and 5.0 eV. Because the model ϵ_2 is discontinuous at 6.0 eV, the KK values diverged rapidly from the appended Aspnes and Studna values above 5.4 eV. A detail of the below-gap region, shown in Fig. 9, demonstrates reasonable agreement between the KK values and previously published index values.[4,8] The KK and experimental values are very close just above the gap where the substrate is opaque and the rotating-analyzer ellipsometer data is accurate. Below the gap the values are also in good agreement, although the experimental data become noisier. The KK model provides a more physically justifiable representation of the below-gap region, because the measurement difficulties in this region are not involved. Note, the KK model did not include experimental ϵ_1 values below 1.4 eV when fitting the high-energy oscillator parameters.

The final "best" set of optical constants is shown in Fig. 10 from 0.5 to 5.0 eV. The ϵ_2 spectrum is broken into two sections: Below 1.32, an exponential decay in absorption coefficient was used, and from 1.32 to 5.0 eV direct SE-fitted values assuming t_{ox}=2.02 nm were used. The ϵ_1 values are from the KK analysis model. These values are virtually identical to the direct SE-fitted values above the gap [Fig. 4(a)] and close to, but smoother than, the direct-fitted values below the band gap (Fig. 9).

VII. CONCLUSIONS

We have used VASE to measure the intrinsic dielectric function of InP from 0.75 eV through the direct gap at 1.35 eV, up to 5.0 eV. Previously published absorption measurements from 1.37 to 1.38 eV were used to determine the overlayer oxide thickness of 2.02 nm. The below gap imaginary part of the dielectric function was modified using an exponential tail to model the absorption roll-off below 1.32 eV. These InP values are demonstrated to be compatible with published pseudovalues assuming an oxide layer of 0.27 nm on Aspnes and Studna's sample. These measurements are also shown to be KK consistent above the band gap and compatible with prism-measured refractive index values below the gap.

ACKNOWLEDGMENTS

We thank F. G. Celii and Y.-C. Kao of Texas Instruments for supplying the InP substrate used for these measurements. This work supported by ARPA Consortium Agreement No. MDA972-93-H-0005.

[1] D. E. Aspnes, in *Handbook of Optical Constants of Solids*, edited by E. Palik (Academic, Orlando, FL, 1985), Chap. 5.
[2] U. Rossow, A. Krost, T. Werninghaus, K. Schatke, and W. Richter, Thin Solid Films **233**, 180 (1993).
[3] W. J. Turner, W. E. Reese, and G. D. Pettit, Phys. Rev. **136**, A1467 (1964).
[4] G. D. Pettit and W. J. Turner, J. Appl. Phys. **36**, 2081 (1965).
[5] H. Burkhard, H. W. Dinges, and E. Kuphal, J. Appl. Phys. **53**, 655 (1982).
[6] D. E. Aspnes and A. A. Studna, Phys. Rev. B **27**, 985 (1983).
[7] P. Lautenschlager, M. Garriga, and M. Cardona, Phys. Rev. B **36**, 4813 (1987).
[8] Pikhtin and A. D. Yas'kov, Sov. Phys. Semicond. **12**, 622 (1978).
[9] R. M. A. Azzam and N. M. Bashara, *Ellipsometry and Polarized Light* (North-Holland, New York, 1977), Chap. 4.
[10] H. Yao, P. G. Snyder, K. Stair, and T. Bird, Mater. Res. Soc. Symp. Proc. **242**, 481 (1992).
[11] G. E. Jellison, Jr., Thin Solid Films **234**, 416 (1993).
[12] W. H. Press, B. P. Flannery, S. A. Teukolsky, and W. T. Vetterling, *Numerical Recipes: The Art of Scientific Computing* (Cambridge University Press, Cambridge, MA, 1988), Chap. 14.
[13] G. E. Jellison, Jr., Appl. Opt. **30**, 3354 (1991).
[14] P. G. Snyder, M. C. Rost, G. H. Bu-Abbud, and J. A. Woollam, J. Appl. Phys. **60**, 3293 (1986).
[15] The exception to this observation is for the extraction of optical constants at one angle of incidence from a single sample where the number of measured values and extracted values are equal. In this case, the model and experimental values are identical, and any systematic errors are passed along in the extracted optical constants which in turn can become sources of systematic errors in analysis of other samples.
[16] G. H. Bu-Abbud, N. M. Bashara, and J. A. Woollam, Thin Solid Film **138**, 27 (1986).
[17] S. Zollner, Appl. Phys. Lett. **63**, 2523 (1993).

Downloaded 04 Dec 2007 to 129.93.17.223. Redistribution subject to AIP license or copyright; see http://jap.aip.org/jap/copyright.jsp

[18] It may be unsatisfying to tie a supposed intrinsic material parameter like dielectric constant to some model assumption (that assumption may be $t_{overlayer}$=0 Å), but this is always the case in a model-dependent measurement technique, such as ellipsometry.
[19] G. E. Jellison, Jr., Opt. Mater. **1**, 151 (1992).
[20] G. E. Jellison, Jr., Opt. Mater. **1**, 41 (1992).
[21] D. E. Aspnes, *Handbook on Semiconductors*, edited by M. Balkanski (North-Holland, New York, 1980), Vol. 2, p. 109.

Downloaded 04 Dec 2007 to 129.93.17.223. Redistribution subject to AIP license or copyright; see http://jap.aip.org/jap/copyright.jsp